PUBLICATIONS OF THE NATIONAL RADIO ASTRONOMY OBSERVATORY
Volume 1 October 1962 Number 14

THE EFFECT OF ATMOSPHERIC RADIATION IN THE MICROWAVE REGION

Torleiv Orhaug*

ABSTRACT

This report deals with the fluctuating component in antenna noise temperature resulting from varying atmospheric absorption along the line of sight of the antenna. The equipment used for observing the fluctuating component at two frequencies -- 3 KMc and 8 KMc -- together with the observing and analyzing procedure is described. A theoretical investigation of the variation in atmospheric brightness temperature resulting from known characteristics of variation in the atmospheric properties is carried out, and it is shown that fluctuations of the order of 0.1 - 0.5 °K may result both from variations in water vapor and from presence of condensed water in clouds. This is confirmed by observations, which show that variations in atmospheric brightness temperature above 1.0 °K may occur for as much as 20 per cent of total observing time at 8 KMc. This fluctuating component is shown to be correlated with clouds, but it is also shown that even in clear weather fluctuations may be encountered. These latter fluctuations probably result from variations in water vapor.

I. INTRODUCTION

The atmosphere is known to influence microwave radio wave propagation in many ways. Refraction of microwaves is dependent upon actual atmospheric conditions: both line-of-sight and beyond-the-horizon signals show instabilities in terms of amplitude and direction-of-arrival fading; atmospheric gradients and rain clouds are known to reflect and scatter radio waves for various atmospheric conditions and frequencies. The influence of various atmospheric conditions upon the sensitivity of the system, however, has not been extensively investigated. The earliest work in this field is that of Dicke, et al. (1946). They observed the atmospheric noise at microwave frequencies, and introduced the celebrated switching technique for improvement of stability. Recently a detailed investigation has been reported by Hogg and Semplak (1961), using a maser at 6 KMc. Both of these investigations were concerned only with the value and slow variation of the atmospheric noise level. Hogg also pointed out that in a low-noise system utilizing a maser the antenna temperature may be of primary limitation for the total system sensitivity. If, however, the variation in the antenna temperature, caused, for instance, by varying atmospheric conditions, occurs during a time which is of the same order of magnitude as the output filtering time of the observing system, then the limiting factor is not only the

*On leave from Chalmers University of Technology, Gothenburg, Sweden.

The National Radio Astronomy Observatory is operated by the Associated Universities, Inc., under contract with the National Science Foundation.

actual value of the antenna noise, but is the added effect of the noise level and of the variation of the noise level. If the receiving system utilizes a rather large output bandwidth (as is the case in radar and communication application), then the noise level will limit the sensitivity. In other applications such as radio astronomy, on the other hand, the output bandwidth is often extremely narrow (of the order of $1 - 10^{-2}$ c/s), and therefore the noise fluctuations are very small. Under such conditions the fluctuation term may be of vital importance for the system sensitivity. The relative importance of the atmospheric noise level and the fluctuation component depends upon the system parameters. Assuming that the fluctuation component has noise-like properties with an rms-value of ΔT_{fluct}, this additional output fluctuation is equivalent to an increase in system noise temperature of approximately

$$T_{syst} \left\{ \left[1 + \frac{\Delta T^2_{fluct}}{T^2_{syst}} B\tau \right]^{1/2} - 1 \right\}$$

since the output fluctuations from the noise of the radiometer and from the atmospheric fluctuations are statistically independent. If, for instance,

$$T_{syst}/\sqrt{B\tau} = 1, \text{ and } \Delta T_{fluct} = 1 \text{ °K}$$

the equivalent increase in system noise temperature is 42 per cent. The fluctuation term may therefore be a limiting factor as far as system sensitivity is concerned, and it therefore is important to undertake a detailed investigation of the atmospheric fluctuation term and thereby gain some information as to the causes of the fluctuation term and the dependence upon atmospheric conditions. The results from a theoretical and experimental investigation of the fluctuation term of the atmospheric noise temperature is discussed here. The importance of atmospheric conditions for microwave radiometry has been reported before. For instance, earlier observations at NRAO using an 8 KMc TWT radiometer on the 85-foot telescope had shown that observations often were heavily disturbed by atmospheric effects (Westerhout 1959).

Section II of this report describes the equipment and observing procedure which were used for studying the atmospheric effects, and in section III an investigation is made of the effects to be expected for the fluctuation component due to various atmospheric conditions. For this investigation the theoretical values for the absorption coefficient at microwave frequencies have been utilized and the fluctuation component to be expected from both water vapor and condensed water has been treated. Section IV contains the observational results from both 8 KMc and 3 KMc. The fluctuation component was partly investigated by pointing the telescope at the pole so that no variations in antenna temperature were caused by sources drifting through the antenna beam. In order to investigate the fluctuation effect at 3 KMc, rather low elevation angles had to be used, and in that case the telescope was parked and the sky was allowed to drift by. Section V is devoted to a discussion of the observational results and concluding remarks.

It should be pointed out that the atmospheric effect described in this report is due to thermal radiation by the atmosphere, and results from the absorption characteristics

of the transmission medium. Another effect may arise from the reactive component of the impedance influencing the phase characteristics of a wave propagating through the medium. For a full discussion of the influence of the atmosphere on microwave radiometry the variations in the reactive properties should also be taken into account. In this report, however, we shall only be dealing with the lossy characteristics of the atmosphere and the effects to be expected from variations in this characteristic.

II. DESCRIPTION OF EQUIPMENT AND OBSERVING PROCEDURE

The observations described in section IV of this report were carried out with modified versions of two TWT switched-load radiometers built by the Ewen-Knight Corporation and described by Drake and Ewen (1958). The main characteristics of the two radiometers are given in Table 1 below.

TABLE 1

CHARACTERISTICS OF RADIOMETER SYSTEMS

Radiometer	Center Frequency	Bandwidth	T_R	Antenna
1	8 KMc	1 KMc	2800	12-foot parabolic dish, 4-foot horn antenna
2	3 KMc	0.2 KMc	1000	85-foot parabolic dish

The 12-foot antenna was used for the 8 KMc observations between December, 1961 and April, 1962, while the 4-foot horn antenna was used in May and June. Both of these antennas were mounted close to the observing house so that the entire receiver system could be kept in the house, thus enabling operation under laboratory conditions. The losses in the waveguide from the antenna to the receiver input were estimated to be 2 db, a value which was also confirmed by measurements. The 12-foot antenna was mounted firmly on the ground in the direction of the pole, and therefore permitted observations of sky noise temperature and fluctuation component only at a fixed elevation angle (38°). The horn reflector antenna of a design similar to the one described by Crawford et al. (1961) was built in order to permit observations at different elevation angles. The pattern of the horn reflector antenna was measured by using the sun as a source. The results of the measurements are shown in Figure 1. The 3 db beamwidths are 2°.0 and 1°.8 for the longitudinal and transverse planes, respectively, and the efficiency is 70 per cent, assuming the sun's brightness to be 24000 °K at 8 KMc (Pawsey 1955).

The aperture of the horn antenna is 1.45 square meters, and the total length of the horn is 3.35 meters. The noise temperature of the antenna when pointing to zenith was measured and found to be 11 °K. Assuming the sky noise contribution at 8 KMc to be 3 °K

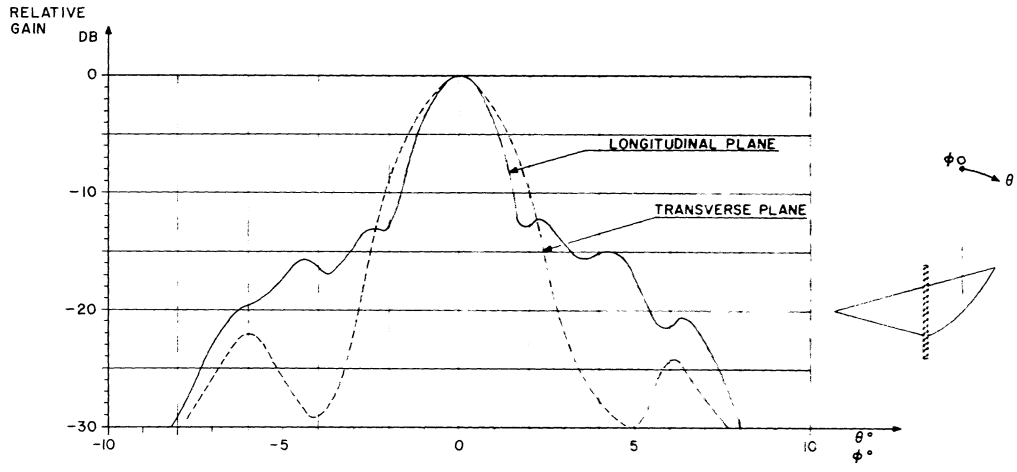

Fig. 1. — Patterns of horn reflector antenna for longitudinal and transverse planes.

in the zenith direction, we obtain an antenna temperature due to losses and spillover of 8 °K. It should be pointed out that this temperature is an upper limit. The actual temperature is extremely dependent upon the value assumed for waveguide losses from the antenna waveguide flange to the point where the temperature is measured.

The front end of the receiver is shown in Figure 3. Close to the horn antenna is a rotating joint to permit rotation of the antenna. The signal from the rotating joint is coupled to one input port of a low-loss waveguide switch, while the other input is connected to a 50-ohm termination (coaxial). Normally, the input of the switch is connected to the antenna waveguide. From the waveguide switch the signal is fed through two directional couplers (L_{D1} and L_{D2}). The first has a coupling of -40 db, and therefore enables a calibration signal of approximately 1 °K to be inserted (from an 10100 °K argon noise source). The second directional coupler has a coupling of -10 db and is fed from an argon noise source through a calibrated attenuator (0 - 40 db). The output of the last directional coupler is then connected to one input port of a ferrite switch (insertion loss 0.3 db). The other input of the switch is connected to a -10 db directional coupler (L_{D2}) and the coupler terminated into a load at room temperature. Noise is added to the antenna channel through directional coupler L_{D1} by adjusting attenuator L_{A1}, so that the total noise in the antenna channel is equal to T_C. The radiometer is then operating under balanced condition. The amount of balancing noise being added to the antenna noise is consequently

$$T_B = T_C - T_A$$

where T_A is the equivalent noise temperature of the antenna output. We have assumed

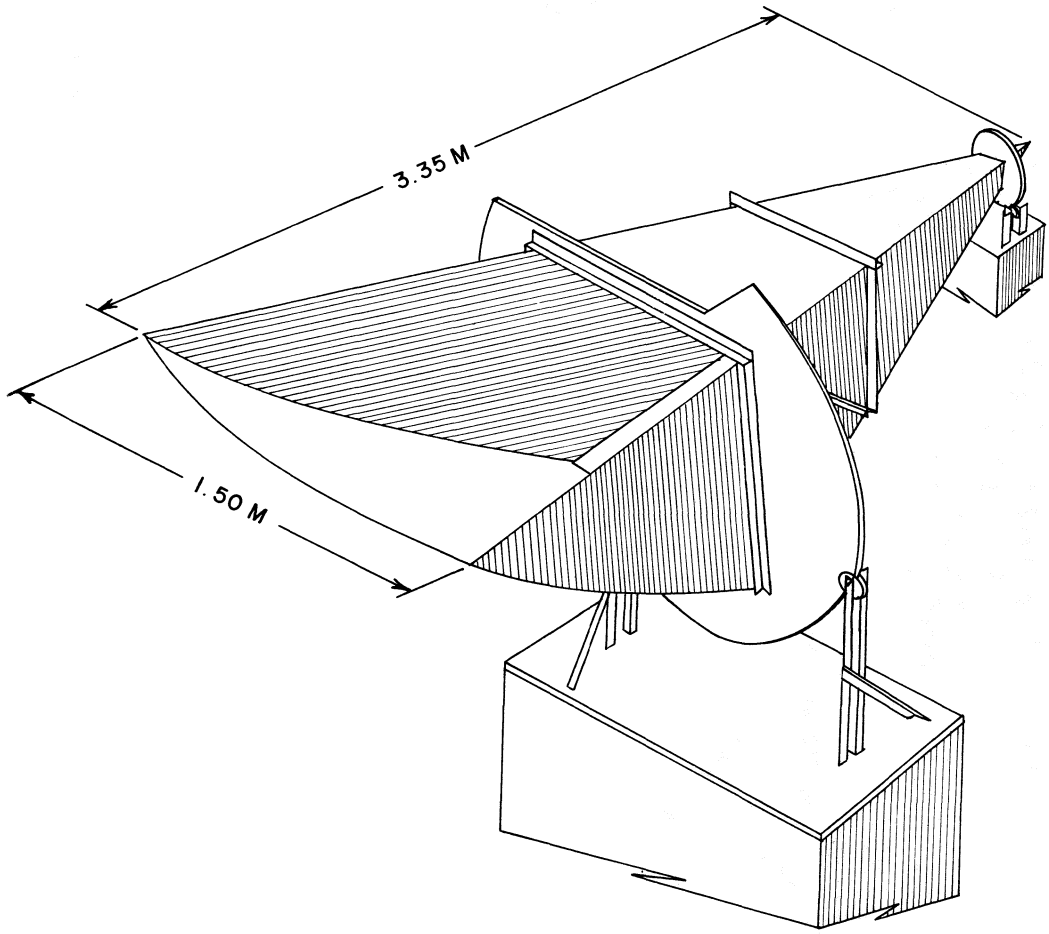

Fig. 2. — Schematic drawing of the horn reflector antenna.

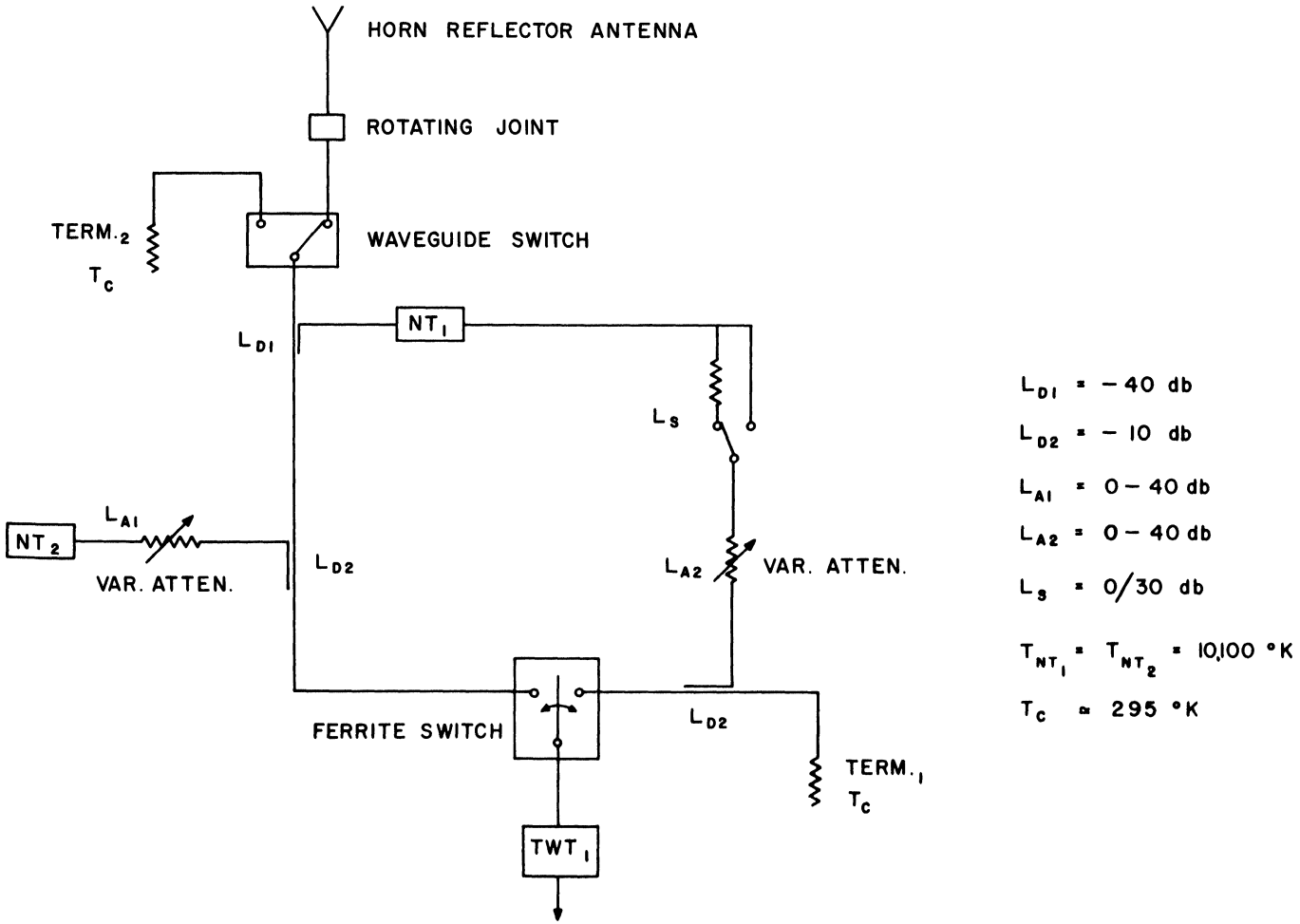

Fig. 3. — Front end of the 8 KMc TWT radiometer.

that there are no losses in the waveguide system between the antenna output and the directional coupler L_{D2}.

In order to make a check of receiver stability performance the waveguide switch is switched into the termination position. The radiometer is now unbalanced since the antenna input to the ferrite switch has an equivalent temperature of $2T_C - T_A$, and therefore the solenoid operated attenuator L_S is energized so the attenuation of L_S is 0 db (compared to its 30 db unenergized value). The attenuator L_{A2} is adjusted so the added noise to the comparison channel is $2T_C - T_A$. In this way the radiometer can be tested under balanced condition with a constant-input noise source.

The 3 KMc radiometer was of a design similar to the 8 KMc radiometer but was not provided with a room temperature load for stability checks. When observations were made by using the 3 KMc receiver, the stability was checked by pointing the dish to the ground and rebalancing the receiver. Such stability runs were made frequently during the observations and only observations which showed negligible or small drift of the receiver conditions were analyzed.

An example of receiver performance at 8 KMc is shown in Figure 4. Observation with input terminated in matched load and observation on the 12-foot antenna is shown. The long- and short-term stabilities are very good. When the antenna is connected, long-term variations of the order of 2 °K and short-term variations of the order of 1 °K are seen to be present. This report mainly deals with the nature of the short-term variations, which have a period of the order of minutes. The long-term variation is partly due to temperature changes of the waveguide from the antenna to the receiver. The waveguide of the 12-foot telescope had a loss of approximately 2 db and most of the waveguide was outdoors and therefore was exposed to temperature variations. The loss of the front-end waveguide of the horn reflector antenna was approximately 1 db and, since the entire waveguide was indoors, the effects of ambient-temperature changes were considerably reduced.

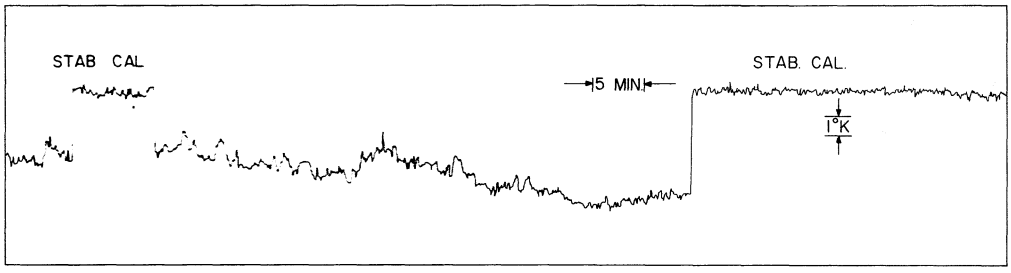

Fig. 4. — Record of 8 KMc radiometer performance and atmospheric noise fluctuations. The scale of effective input temperatures to the receiver is indicated on the record.

III. ATMOSPHERIC ABSORPTION

The present section contains a discussion of the atmospheric noise level to be expected for various meteorological conditions and a more detailed discussion of fluctuations of atmospheric noise. Both large-scale fluctuations due to snow and rain, and small-scale fluctuations due to water-vapor variations and condensed water are treated.

1. Atmospheric Noise Level

The absorption of the atmospheric gases at microwave frequencies has been investigated by van Vleck (1947). The main contribution to the absorption coefficient, α, comes from the presence of oxygen and water vapor in the atmosphere. The corresponding radiation temperature from the atmosphere has been studied by Hogg (1959), among others. The latter author considered the brightness noise temperature from a standard atmosphere having a water-vapor content of 10 grams/m^3 at ground level, and also from a humid atmosphere with 20 grams/m^3. The temperature profile was assumed to be a linear function of height. The radiation temperature from the total atmosphere is

$$T_b = \int_0^\infty \alpha \; T \exp\left(-\int_0^h \alpha \; dh\right) dh$$

where α and T are the absorption coefficient and temperature at the height h. In Figure 5 we have replotted some of the results published by Hogg. The antenna noise temperature is assumed to be equal to the brightness temperature of the sky (assuming only atmospheric contribution), and the antenna temperature is given for different zenith angles for three different frequencies (0.5, 2, and 10 KMc). In addition, for the highest frequency, the effect of increasing the water-vapor content from 10 to 20 grams/m^3 is indicated.

As was pointed out in section I, the noise temperature of the atmosphere directly deteriorates the sensitivity of a radiometer system because the antenna noise is added to the system temperature. As Hogg (1959) pointed out, this effect may be quite serious, in particular for low-noise receiving systems. In order to show what can be gained by using an observing station at a high altitude, Figure 6 shows the antenna temperature as a function of observing wavelength for the zenith direction for different altitudes of the observing site. The model used for this computation was similar to the one used by Hogg. The barometric pressure was assumed to vary with height according to an exponential law, the temperature profile was assumed linear and the water-vapor content was assumed linear (ρ = 5 gram/m^3 at h = 0 km and ρ = 0 at h = 5 km).

From Figure 6 we can see that for an observing station at an altitude of 2 km, the noise temperature is 1.3 °K at 3 cm wavelength, or 43 per cent of the corresponding noise temperature for a station at sea level. The result from observing at a higher altitude is mainly to reduce the contribution of the water-vapor content. This is, of course, due to the height profile we have chosen, which assumes no water-vapor contribution over h_o = 5 km. In practice, the water-vapor height profile may be more rapidly decreasing than the linear profile. The assumption of no water vapor above 5 km is, however, a good approximation.

2. Fluctuation Component Due to Water-Vapor Variations

We are, however, more interested in knowing the different causes for variation in atmospheric temperature. It is obvious that large-scale variations in atmospheric temper-

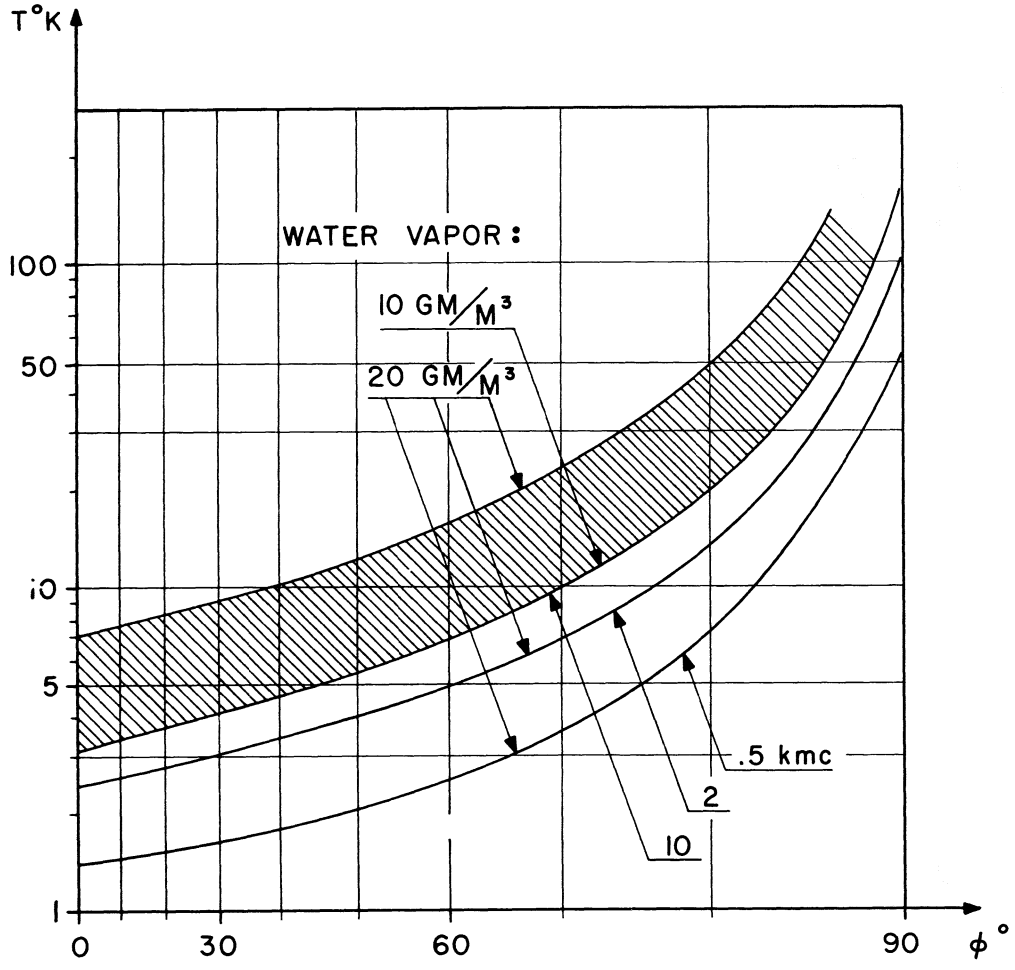

Fig. 5. — Antenna noise temperature T °K due to atmospheric absorption as a function of antenna zenith angle for three different frequencies in the microwave region.

ature can be expected when variations in pressure, temperature, water-vapor density, or in the height profiles take place. These changes are not, however, expected to occur over a short period of time and they will therefore cause only a slow variation in the atmospheric temperature. If we, on the other hand, assume that a change in absorption coefficient α occurs over a limited height interval ΔL, the corresponding variation in brightness temperature will be approximately

$$\Delta T = Te^{-\alpha \Delta L}(\Delta \alpha \Delta L)$$

where the absorption-coefficient value is $\alpha + \Delta\alpha$ in the interval ΔL. Here $\Delta\alpha$ is a function of pressure, temperature, and water-vapor variation. The most significant parameter in this case is the variation of water vapor. The best information concerning the spatial variation of this parameter is that obtained from refractometer measurements. The refractometer measurements give the variation of the index of refraction; the most important parameter contributing to this variation is the variation of the water-vapor content. Thus, we can use the observed variation in index of refraction to deduce the cor-

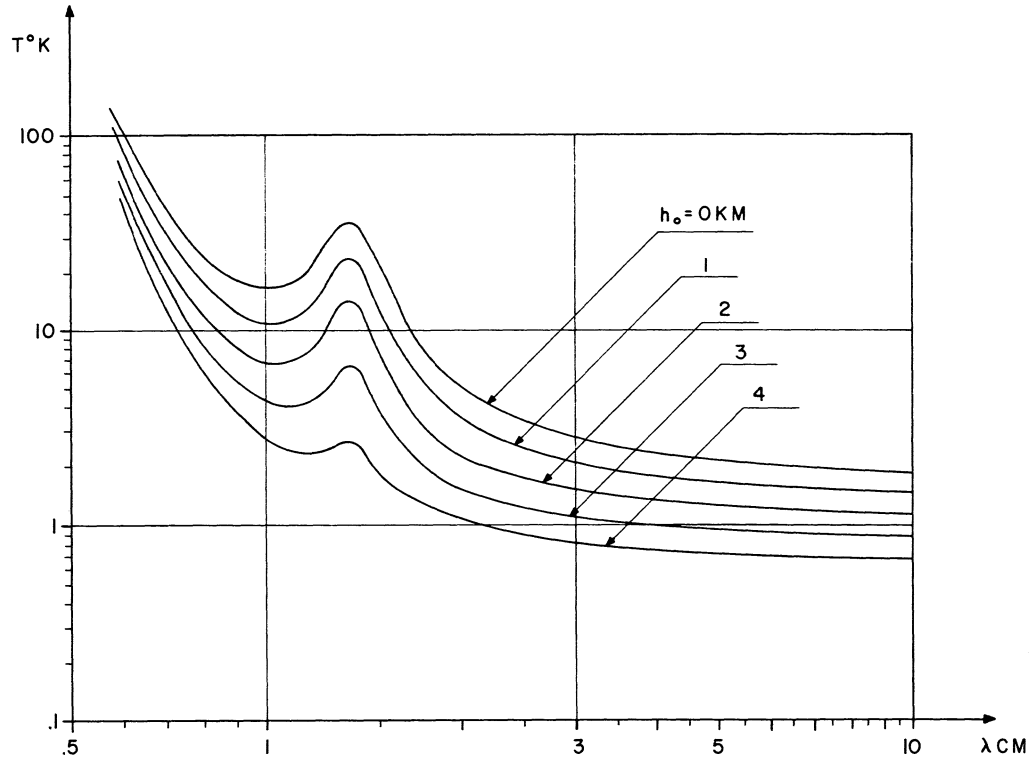

Fig. 6. — Antenna temperature from atmospheric noise in the zenith direction as a function of wavelength given for different altitudes h_0 of the observing station.

responding variation in water-vapor density. The index of refraction, n, is

$$n = 1 + \frac{79}{T} P - \frac{10e}{T} + \frac{3.8 10^5}{T^2} e \; 10^{-6}$$

where P is the total pressure in mb and e is the partial water-vapor pressure. It is convenient to introduce the parameter, N, the refractivity, where, $N = (n-1)10^6$ and assuming that variation in N is caused only by variation in e, which is a good approximation in practice, we have

$$\Delta N = 4.2 \; \Delta e$$

assuming T = 300 °K. Refractometer measurements at different altitudes have given as a result that large-scale variations in N of the order of 50-200 N-units can occur in the first 5 km of the earth's atmosphere (Gerhardt 1955). For $\Delta N = 200$ the corresponding e-variation is $\Delta e \simeq 50$ mb. The absorption coefficient for water vapor is directly proportional to the water vapor density, ρ gram/m^3, and therefore

$$\Delta\alpha = \alpha \frac{\Delta\rho}{\rho} = \alpha \frac{\Delta e}{e} .$$

If the absorption coefficient is given in nepers (α_n), then the corresponding change in brightness temperature is

$$\Delta T_b \simeq T e^{-2\alpha_n \Delta L} (2\alpha_n \Delta L)$$

and assuming $\alpha = 0.01$ db/km $= 1.15 \cdot 10^{-3}$ neper/km, $\rho = 5$ gram/m^3, T = 250 °K, p = 600 mm Hg and $\Delta e/e \simeq 0.2$, we obtain for $\Delta L = 1$ km

$$\Delta T_b \simeq 0.5 \text{ °K} .$$

From this we can see that variations in the water vapor density of the order observed in the atmosphere may produce changes in the atmospheric brightness temperature of the order of 1 °K. Another question is whether the horizontal extension of this irregularity is so small that the duration of the variation in the antenna temperature is minute enough to be serious (of the order of minutes). Little information is available on this point.

3. Fluctuation Component Due to Condensed Water

We shall next turn to consider the effect of water in condensed form in the atmosphere, where we shall be concerned with the effect of rain, snow, and condensed water in clouds. The microwave absorption by precipitation particles has been investigated, both theoretically and experimentally, and the most detailed work in this field is the one by Gunn and East (1954). They utilized the scattering theory for spherical particles developed by Mie and Stratton, and pointed out that only for $\lambda > 10$ cm can the simple Rayleigh scatter ap-

proximation be used for all raindrop sizes. For higher microwave frequencies the scattering, and thereby the attenuation, depends critically upon the diameter of the raindrops as well as the rate of rainfall R. The absorption values published by Gunn and East have been replotted in Figure 7, and from the absorption values the increase in brightness temperature for a homogeneous rain front of different thicknesses, d, has been computed. For the computation of the brightness temperature the assumption was made that the temperature of the raindrops is 290 °K. The absorption is somewhat dependent upon temperature, but little data are available concerning this dependence. On the other hand, the largest uncertainty in using the data in Figure 7 is the assumption of a homogeneous rainfall. This is certainly an oversimplification, but nevertheless the data in the figure may be of some help for estimating the order of magnitude of the expected variation in brightness temperature for various rainfall conditions.

Let us next consider the expected temperature from snow. Dry snow may either be in the form of ice crystals or flakes. For both forms the following relation exists between the snowfall R in mm of water per hour and Z, the summation of the sixth power of the diameter of the water drops:

$$Z = AR^{\beta};$$

β is here approximately 1.6 and A = 500 for ice crystals and A = 2000 for flakes. The

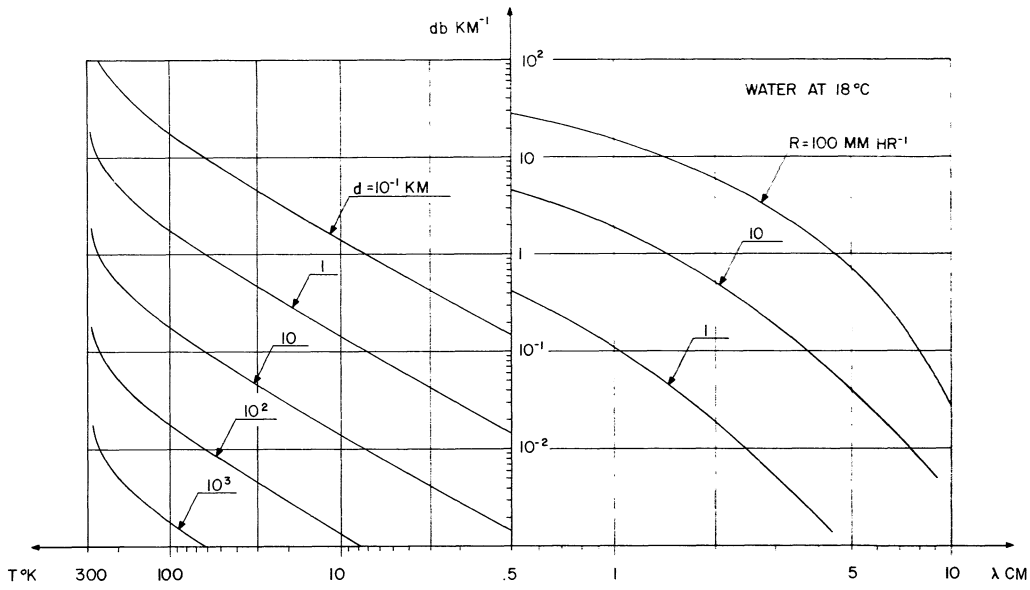

Fig. 7. — Absorption curves for different rates of rainfall R, and brightness temperature T °K for different thicknesses d of a homogeneous rain front.

absorption in db per km for snow is approximately

$$\gamma = B \cdot 10^{-3} \frac{R}{\lambda} \text{ db/km}$$

where $B \approx 2.24$ for 0 °C. Based on this equation we have computed in Figure 8 the expected absorption as a function of wavelength for different snow rates, and also the brightness temperature to be expected from a homogeneous front of snow having the thickness of d km. The dependence of both the absorption and the brightness temperature upon the temperature of the snow particles is indicated in the figure. From the data presented in

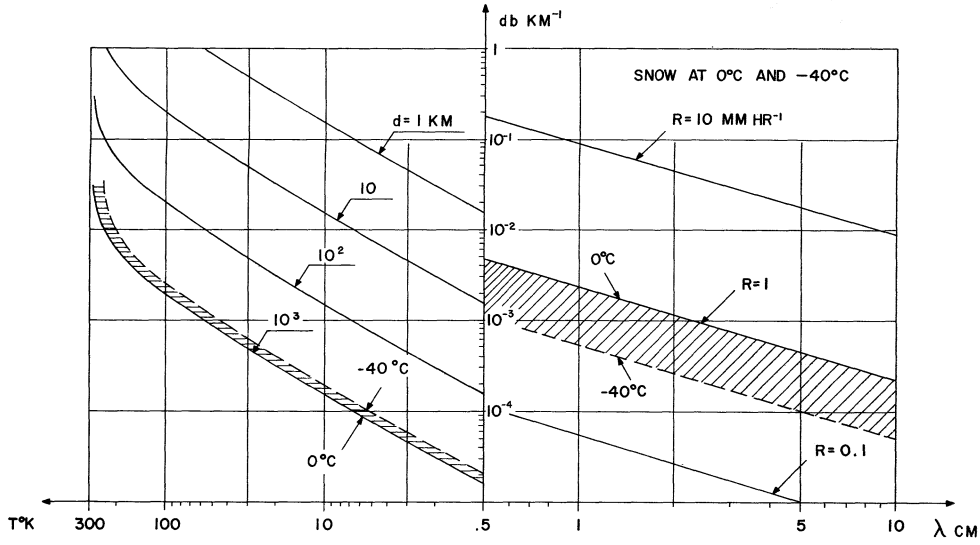

Fig. 8. — Absorption curves for different snow rates R (mm of water per hour) and brightness temperature T °K for different thicknesses d of a homogeneous front of snow. The dependence upon snow temperature is indicated in the graph.

Figures 7 and 8 we can see that for a rainfront of a medium intensity (R = mm/hr) we can expect an increase in sky temperature between 20 and 200 °K for a thickness of the rainfront between 1 and 10 km for an observing wavelength of 3 cm. Temperature increases of more than 20 °K should therefore be observed frequently. For a reasonable snowfall (R = 1 mm/hr) the expected rise of temperature is of the order of 0.7 to 7 °K for a snow front between 10 and 100 km (at 0 °C). That is, the expected rise of temperature from a snow front is much less than that from a rain front. The influence of both rain and snow is supposed to be of minor importance to radio astronomy, since the total time of occurrence is relatively short and also because observations during such conditions are often made difficult for other reasons.

Next we shall consider the influence of clouds. For droplet size in clouds, the Rayleigh scatter approximation is valid for $\lambda > 3$ mm, that is, for the whole frequency range we are discussing. The absorption formula is therefore dependent only upon the liquid-water content (M gram/m^3) and is independent of the drop-size distribution. The absorption values given by Gunn and East are presented in Figure 9, together with the brightness temperature for different cloud sizes. From Figure 9 we find that a cloud

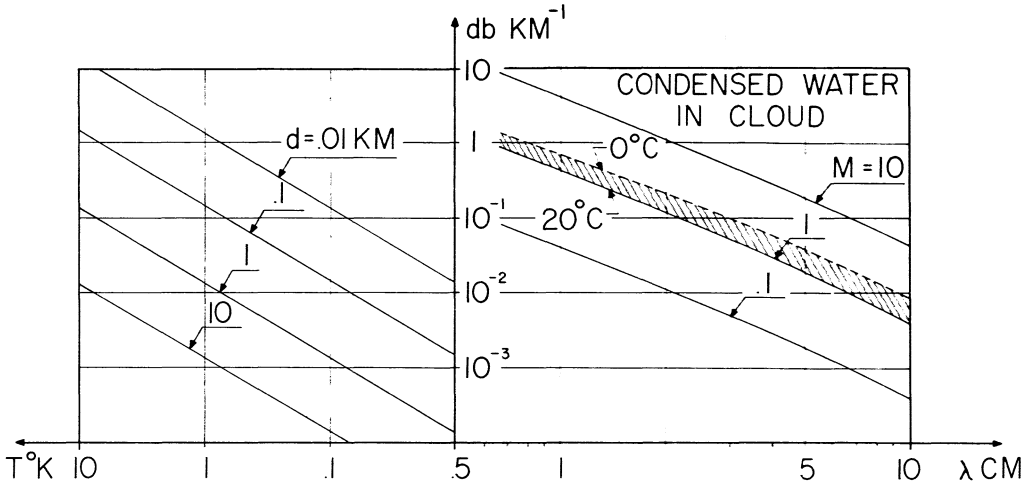

Fig. 9. — Absorption curves for different water content M gram/m^3 and brightness temperature for different cloud sizes d..

having a water content of 1 gram/m^3 and having a dimension of 100 m in the line-of-sight direction will make a contribution of 0.1 °K to the brightness temperature at 3 cm. Figure 9 is given for low-level clouds where the condensed water is in liquid form. It is also of interest to find the expected temperature from high-level clouds where the water is found in solid form. Gunn and East have likewise given the absorption for this case in the microwave region, and the results together with the expected brightness temperature are shown in Figure 10. We see that the expected rise of temperature from an ice cloud is approximately 15 times smaller than that to be expected from a liquid-water cloud.

In order to be able to draw more definite conclusions concerning the variation of atmospheric brightness temperature, a discussion of the cloud height, the cloud size, and the equivalent liquid-water content is needed. In Table II the classification of the different types of clouds is shown, together with their characteristic dimensions. This information is given by Ludham and Mason (1957). The cirrus-cloud type is a high level formation of feathery shape. The stratus formation is a larger type, and the cumulus formation is a heap-type cloud with base at least 1 km from ground level. The table shows that the vertical dimension is between 1 and 10 km.

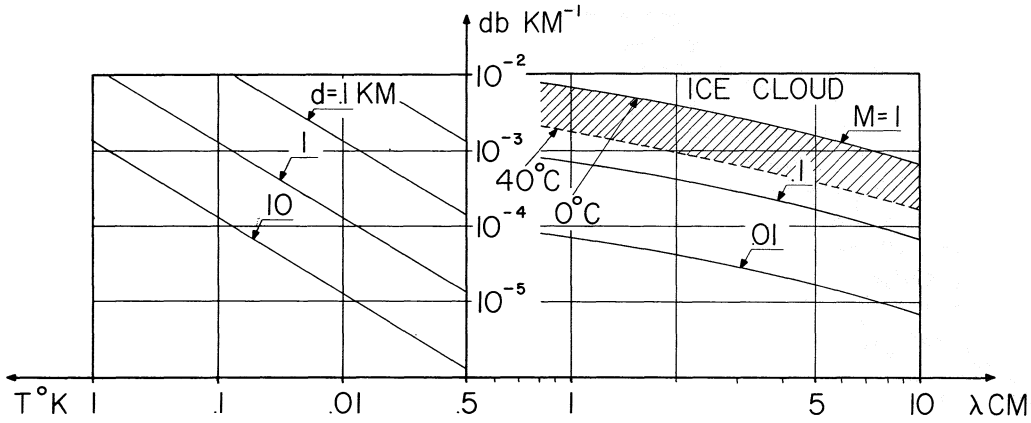

Fig. 10. — Absorption curves for ice clouds as a function of wavelength for different equivalent water content M gram/m^3 and brightness temperature for different cloud sizes d.

The behavior of the absorption for 0 °C and -40 °C is depicted.

TABLE 2

CLASSIFICATION OF CLOUDS

Name	Height km	Dimension in km		Type
		Horizontal	Vertical	
Cirrus Cirrostratus Cirrocumulus	6-13	10^3	10	High level cloud
Altostratus	2.5-6	10^3	10	
Altocumulus		10^3	10	
Stratocumulus	up to 2.5	10^2 - 10^3	1	
Nimbostratus		10^3	10	Precipitating cloud
Cumulus	1-10	1	1	
Cumulonimbus		10	10	Precipitating cloud

Measurements of liquid-water content are fairly rare because of the difficulties of making such measurements. Measurements by Weickmann and Aufm Kampe (1953) and Zaitsev (1950) are shown in Figure 11. The former observations were taken in cumuliform clouds and the latter in cumulus-congestus forms. Figure 11 shows that at least for the observed cumulus clouds a reasonable mean value for the liquid-water content throughout the cloud is between 1 and 2 gram/m^3. The liquid-water content can also be computed from the visibility within the cloud, and such measurements have been made by Aufm Kampe (1950). The results are shown in Table 3. The maximum water content may be found both at the top and the base of the cloud. Even though there is more moisture available for condensation at lower level, strong vertical currents within the cloud may carry aloft cloud particles. The water vapor in the cloud can for all practical purposes be considered saturated. This means that cumulonimbus clouds with a base temperature of about 20 °C have a water-vapor content of 17 gram/m^3. The liquid water content will remain approximately constant with altitude up to about 7 km, while the water-vapor content decreases rapidly with height, because of decreasing temperature (Cole 1960). Few studies have been made of clouds above 7-8 km. The condensed water in these clouds will usually be composed of ice crystals having a solid water content of less than 0.1 gram/m^3. When condensed water is also present the total content is between 0.1 and 1.0 gram/m^3. This does not apply to cumulonimbus formations, however, in which case the total content of water (solid and liquid) may attain a density of 10 gram/m^3 at 8 km (Cole 1960). In addition to the effect of condensed water in clouds, the effect that the relative humidity in the cloud is higher than that of the surrounding should be accounted for. Brewer and Harrison (1944) have made observations of relative humidity up to 8 km, and their conclusion was that any relative humidity between 30 and 90 per cent is about equally common outside the clouds. The actual increase in liquid water content in the cloud compared with the increase in its surrounding depends also upon the temperature.

TABLE 3

AVERAGE WATER CONTENT IN CLOUDS
COMPUTED FROM VISIBILITY OBSERVATIONS

Cloud Type	M gram/m^3
Cumulus congestus	2.5
Fair weather cumulus	0.5
Stratocumulus	0.2
Stratus	0.2-0.3
Altostratus	0.2

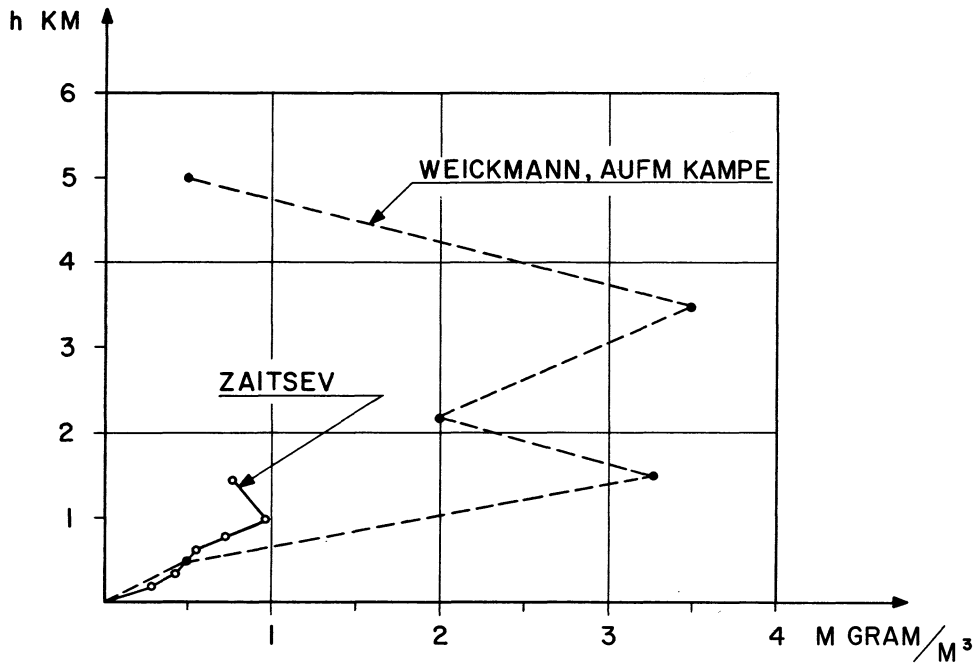

Fig. 11. — Liquid water content as a function of height above cloud base according to Weickmann and Aufm Kampe and according to Zaitsev.

IV. OBSERVATIONAL RESULTS

In this section a résumé of the main observational results of the investigation of atmospheric noise will be given. The observations were made at two frequencies -- 8 KMc and 3 KMc, respectively (3.75 cm and 10 cm wavelengths). The 3.75 cm observations were carried out during the period December, 1961 - June, 1962, and the 10 cm observations during March and April, 1962. For the 3.75 cm case, observations of noise level during precipitation and also observations of the fluctuation component during non-precipitation conditions will be presented. The 10-cm data contain only the fluctuation component for different elevation angles.

1. Noise-Level Variation During Precipitation

The 3.75 cm observations were carried out continuously so that a considerable number of occasions of noise variations during snow and rain were recorded. Since no measurement of rate of snowfall was made, only the noise data during rain will be discussed here. The rate of rainfall was recorded by using a tipping bucket rain gauge. Some examples of noise level variations during rain conditions are presented in Figures 12 and 13. Figure 12 shows a record from February 11, 1962, where the maximum noise level, which is of the order of 10-17 °K, occurs after the maximum phase of the rain. The rate of rainfall was only 1 mm/hr. The noise calibration is referred to brightness temperature by taking into

account the losses in the front-end of the receiver and the efficiency of the antenna. Figure 13 shows a record of a similar type with the maximum in noise level occurring more than half an hour before any rain has started to fall at the observing station. The maximum increase in brightness temperature is of the order of 25 °K. Both this latter and the previous record show the variation in noise level associated with the rain front to be regularly increasing and decreasing with time; and also the rain area passing the station seems to be rather homogeneous as judged from the variation of rate of rainfall with time. The two following Figures (14 and 15) show, however, different features. The records from March 21 and from April 29 show rapid variations in noise temperature, and this variation is closely correlated with variations in rain intensity with the maximum of the two variations occurring at very nearly (within a few minutes) the same time. The maximum increase in noise brightness temperature is approximately 50 °K. The conclusion which can be drawn from this is that appreciable increases in noise level can occur during rain storms, and often the variation in noise level is directly correlated with the rate of rainfall at the observing site. At other times, on the other hand, the maximum in noise level occurs even before the rain has started to fall. These conclusions are similar to the conclusions which Hogg (1961) made from observations at 6 KMc. He suggested the time difference in noise level maximum and rainfall maximum to be due to the slope of the rain column.

Another source which could contribute to the observed intensity is radiation from lightning. This effect has, however, a characteristic feature which can easily be distinguished on the record. The records presented in Figures 12 through 15 are not believed to have been influenced by this effect, and it is therefore considered that they directly represent the thermal radiation from rain fronts. A résumé of the increase in noise level in terms of brightness temperature observed during rain condition is presented in Figure 16. The maximum increase in brightness temperature is plotted against the maximum rate of rainfall for various rainstorms. The two theoretical curves for 3.75 cm wavelength which are shown on the same diagram represent the expected noise temperature from a rain front of 10 and 5 km thickness along the line of sight, respectively, and are taken from the data represented in Figure 7. The larger thickness is chosen so that the theoretical values should correspond to the maximum points in Figure 16. The observed noise levels are all seen to agree fairly well with the theoretical curves. The noise levels recorded during a small rate of rainfall are, however, seen to fall above the theoretical curve. Such a behavior would be expected if, for instance, the rainstorm with smaller intensity has a larger dimension along the line of sight than that of the rainstorms with a higher intensity. It is interesting to compare the average size of the rainstorm to be expected from the data presented here with sizes found by other observations. Radar observations of rain have given the horizontal and the vertical distribution of the amount of rain water, and results of these observations have been published by Langille (1950). He found for one occasion that the horizontal dimension of the rain front was approximately 5 km and the vertical dimension 3 km. This agrees within the order of one magnitude with the results presented here for noise-level variation during rain.

2. The Fluctuating Noise Component

As was pointed out in the introduction, the main purpose of this report is to show that the atmospheric noise level has a fluctuation component which often is a serious

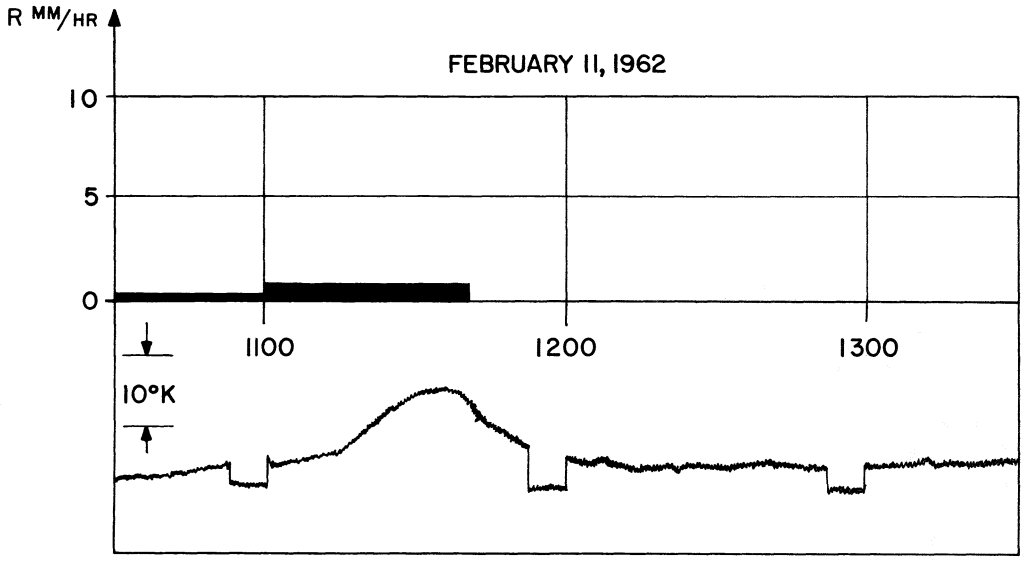

Fig. 12. — Increase in noise level during light rain, February 11, 1962.

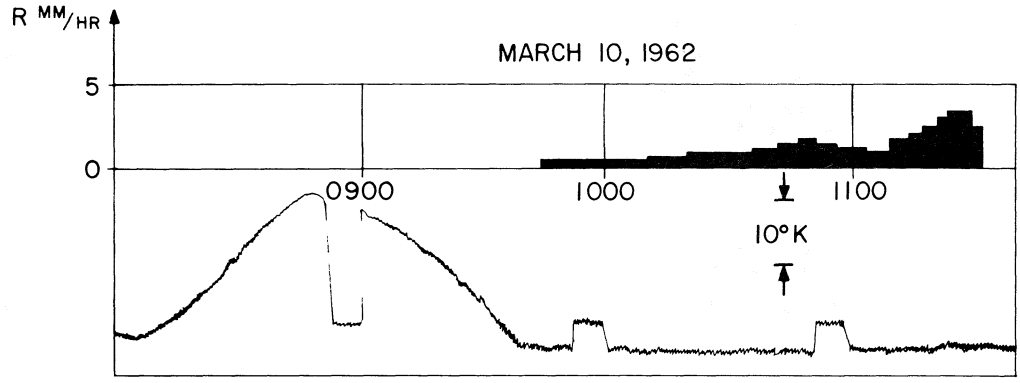

Fig. 13. — Increase in noise level during light rain, March 10, 1962.

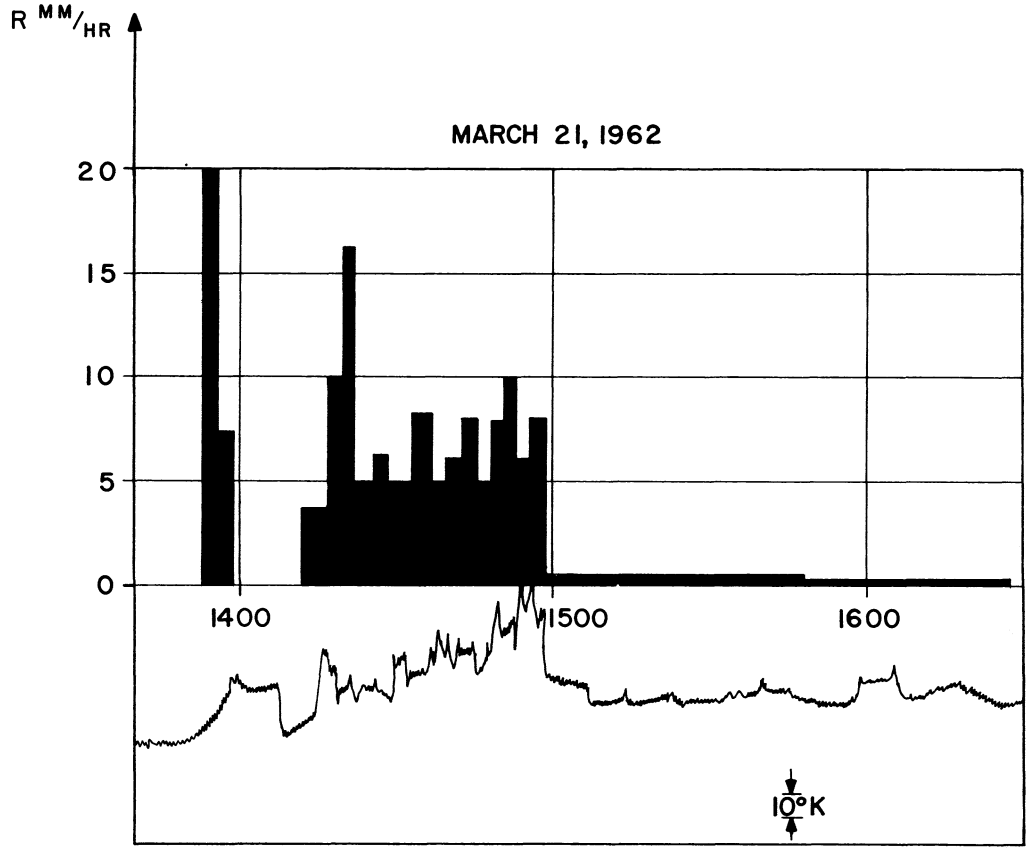

Fig. 14. — Increase in noise level associated with heavy rain on March 21, 1962.

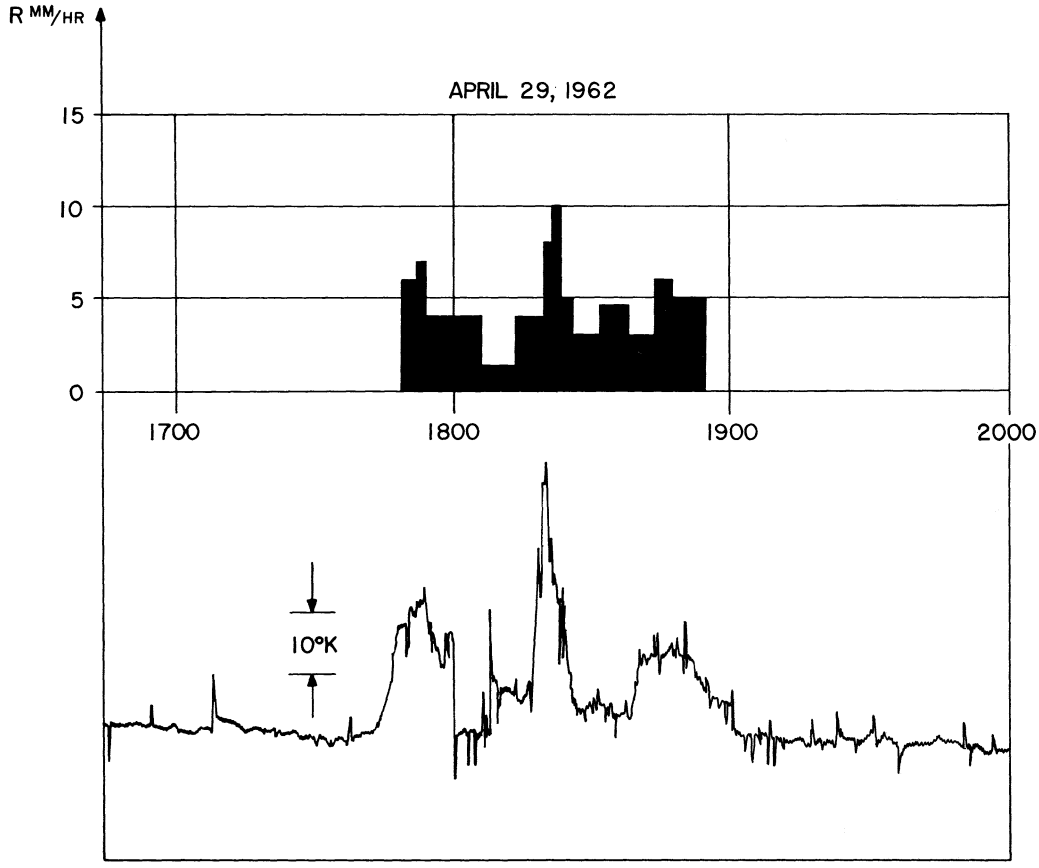

Fig. 15. — Increase in noise level associated with moderate rain on April 19, 1962.

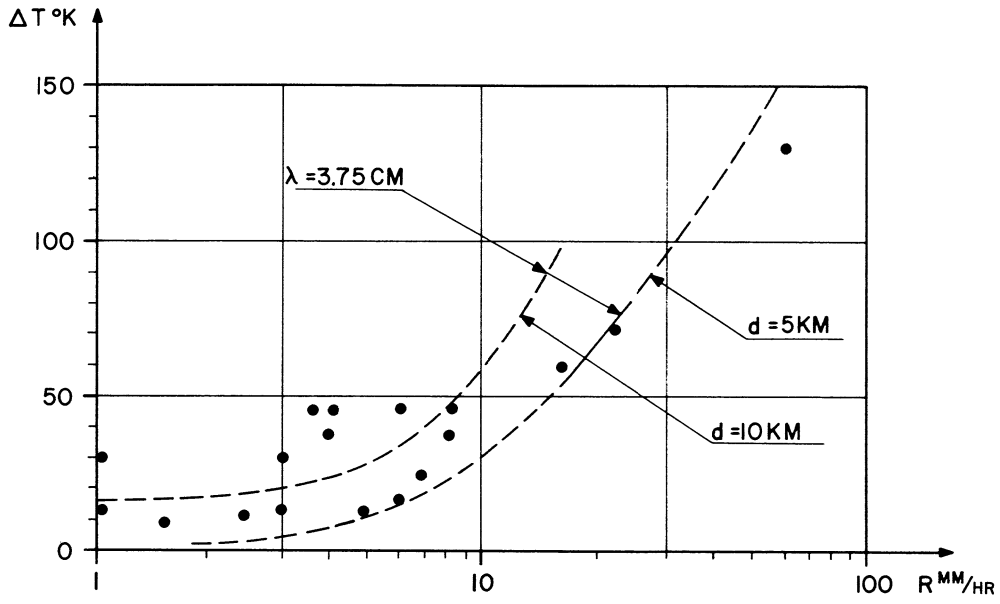

Fig. 16. — Increase in brightness temperature recorded during rainfall as a function of rate of rainfall.

limitation for radiometric observations. The results which are to be presented here come mainly from 8 KMc observations using a 12-foot parabolic antenna pointed at zenith angle of 52° (direction of the pole). Some observations made at 3 KMc using an 85-foot parabolic antenna were also carried out.

a. 8 KMc observations

The 8 KMc observations were carried out between December, 1961, and June, 1962. A total of about 2000 hours of successful observing time was analyzed.

In Figures 17 to 20 are shown selected records representing various conditions. The record from February 4 (Fig. 17) is a record with a very small fluctuation. The temperature scale shown on the record represents brightness temperature, and the stability calibration is seen on the record for 5 minutes every hour. The slow decrease in noise level of the order of 15 °K is associated with a decrease in ambient temperature of 3 °C during the same period of time. Both the long- and the short-term stability of the receiver are seen to be better than 0.5 °K. The sky was almost clear (sky cover 1/10) and the temperature was just below freezing. The next record (Figure 18, February 5), on the other hand, shows a record of a different nature. Starting at a fairly constant level (0900-1000) the noise level later shows long- and short-term fluctuations. The long-term fluctuations have a period of the order of 1 h and an amplitude of 5 °K. It is interesting to note that at 0800-0900 the sky cover was only 2/10, while at 1300

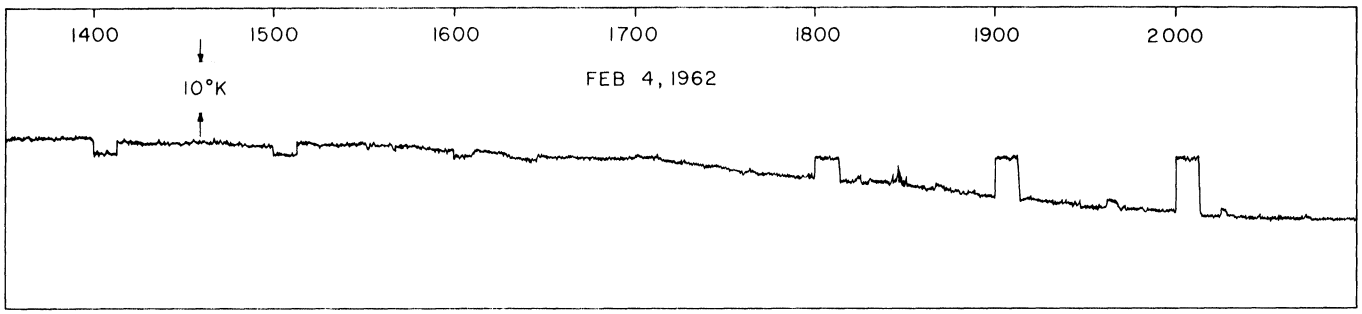

Fig. 17. — Record of 8 KMc atmospheric noise level showing no fluctuations. (February 4, 1962).

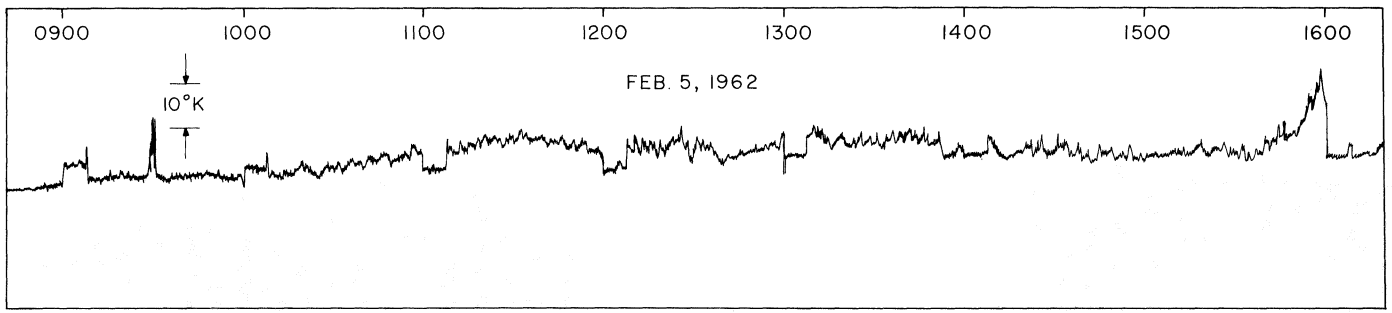

Fig. 18. — Record of 8 KMc atmospheric noise level showing short-term fluctuations of the order of 5 °K. Average sky cover 5/10. (February 5, 1962).

it had changed to full cover (10/10). The temperature was between +2 and +10 °C. The record from April 21 (Figure 19) is of a type similar to the last one discussed. But the general trend is that the fluctuations get less and less intense and disappear at around 1700. Also, the noise level varies about 15 °K, while the ambient temperature varies 14 °C. The small-scale fluctuations have an average period of 8 - 10 min, and the peak-to-peak amplitude is 1-1.5 °K. It should be noted that the sky was clear all through the day. The last record (June 6, Figure 20) also shows brightness-temperature fluctuations of the order of 2 °K having periods of 2 - 5 minutes. During the middle of the day the sky cover was 8/10. The cloud cover decreased to 5/10 at 1500, and correspondingly, the fluctuation component decreased in intensity. Before 1200 the stability calibration was run for 30 min, and the short-term stability is seen to be better than the receiver noise fluctuations or smaller than 0.25 °K. The four records just discussed clearly show that the noise level often has superimposed a fluctuation component which may have a peak-to-peak amplitude of several °K in brightness temperature. The records also clearly show that this fluctuation component is not due to receiver instabilities (which in fact would have looked very similar to the fluctuations just discussed).

Only such observations that by means of the stability calibration could be judged as having a long- and short-term stability better than 0.5 °K were used for analysis. From the records the time interval was estimated during which the fluctuation component was within the amplitude ranges of 0.5-1.0, 1.0-2.0, 2.0-5.0, 5.0-10.0 °K. This was done for four intervals throughout the day (00-06, 06-12, 12-18, 18-24). The temperature ranges refer to the input to the receiver; these ranges were later referred to brightness temperature ranges. From the estimated time intervals, the distribution function was calculated for each month, both for the four different intervals throughout the day and for the entire day. The distribution function gives the average percentage of time during which the fluctuation component exceeded a certain brightness temperature. In Figure 21 and Figure 22 are shown the distribution functions for different sections of the day and for different seasons.

Fluctuations occur with equal probability during nighttime and during daytime. But there seems to be a slight difference in the distribution function as a function of the season, as judged from Figure 22. The fluctuation level is higher during spring-summer (April and June) than during late winter (February and March) with mid-winter (December and January) falling between. The data can, however, not be said to give a very significant conclusion as to the seasonal dependence of the fluctuation component.

The distribution function of the fluctuation component from all the experimental data covering the period December, 1961-June, 1962 is presented in Figure 23. The important result of the work presented in this report is summarized in this graph, and the main point of interest is that at 8 KMc the fluctuation component was observed to exceed approximately 1 °K brightness temperature on the average 21 per cent of total observing time. Fluctuations in brightness temperature exceeding 4.5 °K occurred only during 1.3 per cent of total observing time, showing that the amplitude of the fluctuation rapidly dropped off. There is every reason to believe that fluctuations having a brightness-temperature variation of less than 1 °K occur more frequently than those reported here. From the trend of the distribution curve presented in Figure 23 it seems that fluctuations exceeding about 0.1-0.2 °K are present at all times. This means that for a particular

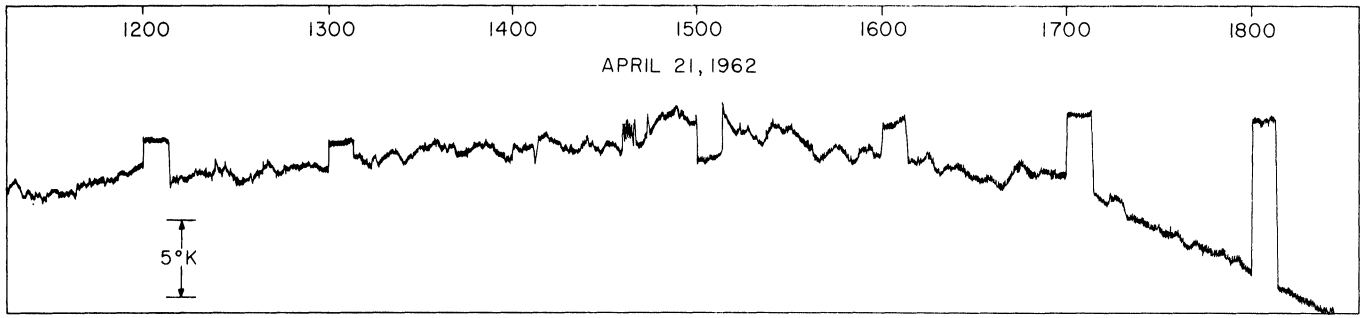

Fig. 19. — Record of 8 KMc atmospheric noise level showing short-term fluctuations of the order of 1 °K. No clouds. (April 21, 1962).

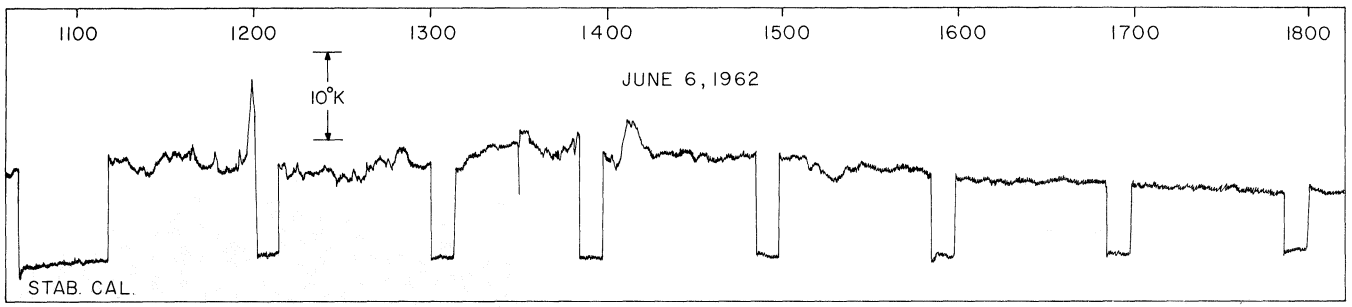

Fig. 20. — Record of 8 KMc atmospheric noise level showing short-term fluctuations of the order of 3 °K. Average sky cover 6/10. (June 6, 1962).

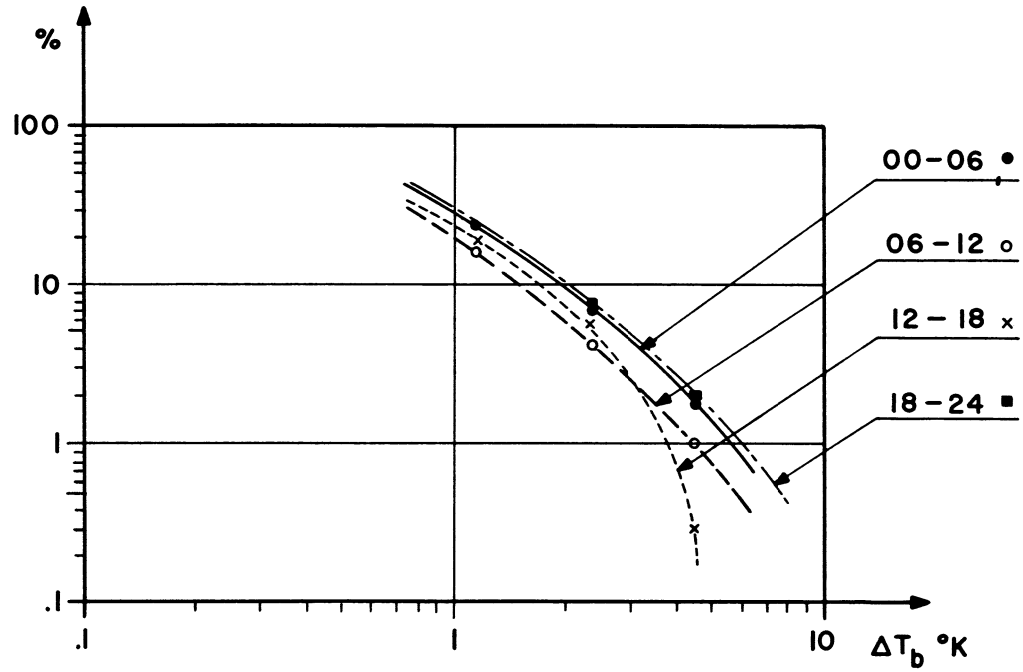

Fig. 21. — Distribution functions giving average percentage of time during which fluctuation component exceeded a certain brightness temperature. The data are divided into sections of the day with six hours in each section.

observing frequency there exists a certain background-fluctuation level, and this point has very great importance for radioastronomical observations. From the data presented here it is difficult to make a very certain guess as to the absolute value of this background-fluctuation level.

The four records presented in Figures 17 through 20 indicate a correlation between the fluctuation component and the presence of clouds. The cloud coverage was estimated several times a day, and Figure 24 shows a correlation plot between the average value of the sky cover and the precentage of the total observing time between 06 and 18 when the fluctuation component exceeded 1.15 °K brightness temperature (corresponding to 0.5 °K at the input to the receiver).

This diagram shows a positive correlation between occurrence of clouds and occurrence of fluctuation in brightness temperature, but it is interesting to note that a certain value of cloud coverage defines more an upper limit of the occurrence of fluctuation than a particular value. This may be explained by the fact that a particular value of cloud coverage does not uniquely define the variation in brightness temperature since the clouds for a particular coverage may be concentrated in layers or be distributed in separate cloud patches. Obviously, the layer-type clouds would exhibit less variation in atmos-

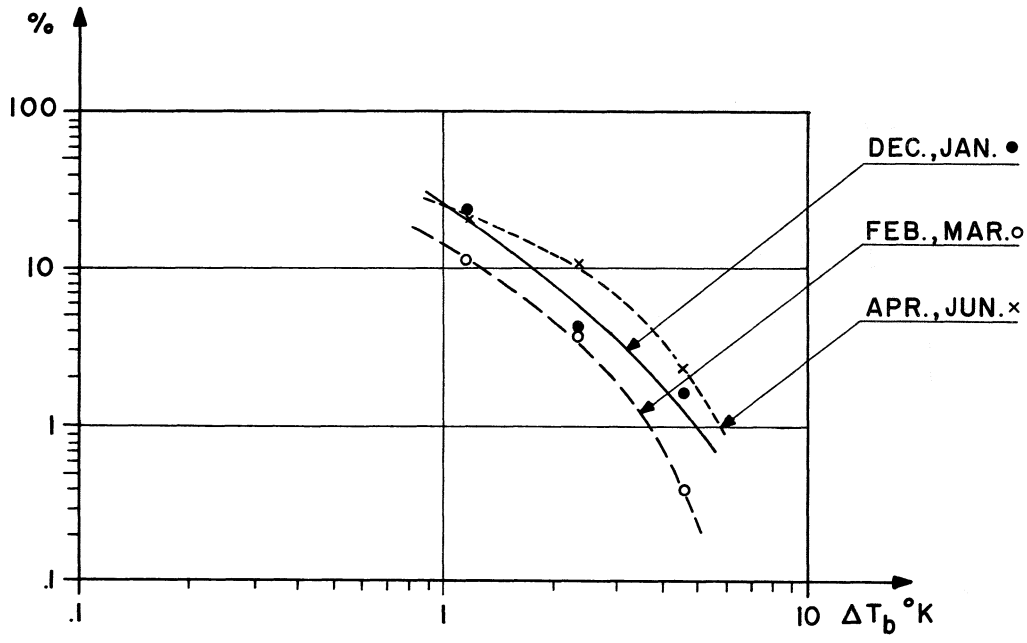

Fig. 22. — Distribution functions giving the average percentage of time during which the fluctuation component exceeded a certain brightness temperature. The data are divided into sections of the year with two months in each section.

pheric attenuation and therefore less variation in brightness temperature. An attempt to find difference in correlation by distinguishing between different seasons and by distinguishing between different types of cloud gave negative results. This may, however, also be due to the finite amount of data available. A lack of correlation was also found by comparing the monthly average of occurrence of fluctuations with monthly average of cloud coverage for a meteorological station in Elkins, 40 miles from Green Bank.

In order to make a more detailed investigation of the dependence between occurrence of clouds and occurrence of fluctuations, the sky in the direction of the antenna beam was watched, and a marker was put on the record every time a cloud passed the antenna beam. The two observations which were carried out are shown in Figure 25 and Figure 26.

The observation of June 23 (Figure 25) was done at two different zenith angles ϕ (indicated on the record). The times when the direction of the antenna beam intersected passing clouds are marked on the record with black areas. The first cloud passage is associated with a slight increase in brightness temperature of the order of 0.5 °K, while the second passage did not have any appreciable effect at all. The third passage is correlated with an increase in brightness temperature of approximately 0.8 °K, and the third passage with 1.5 °K. The reason for the long-term variation between 1520 and 1545 is not known; the variation in antenna temperature was not correlated with any

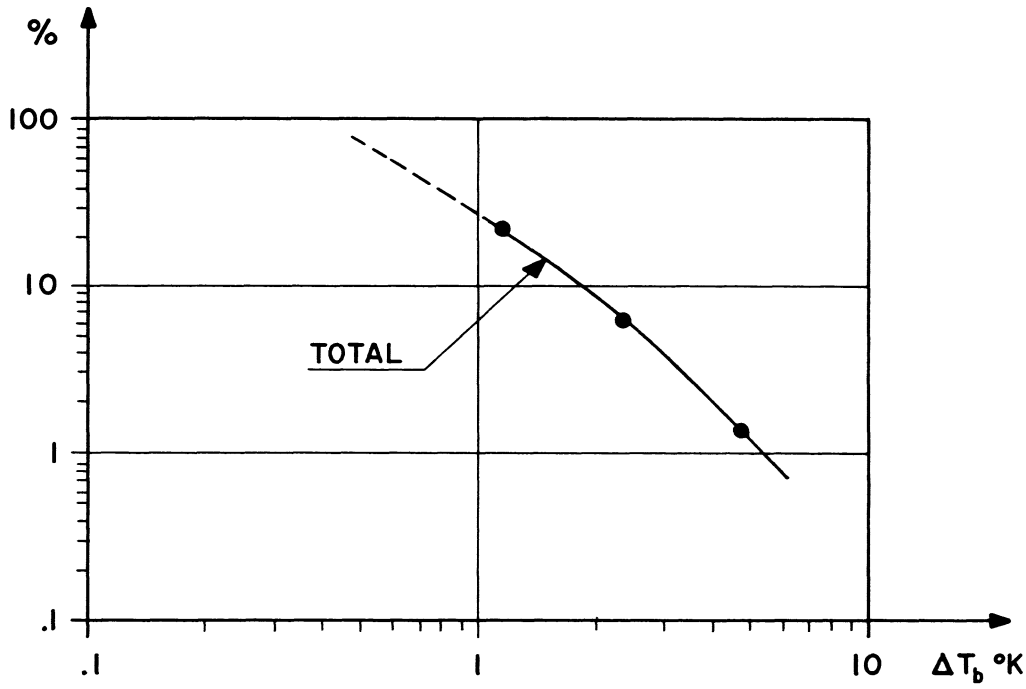

Fig. 23. — Distribution function giving the average percentage of time during which the fluctuation component exceeded a certain brightness temperature. Total material: December 1961-June 1962.

visible event. An even closer relation between cloud passage and noise variation can be seen on the record of June 25 (Figure 26). The first passage is associated with an increase in noise temperature of 1.5 °K and the third one is associated with an increase of 2 °K. The clouds were of the cumulus type. It is interesting to note that the second cloud passage is not associated with any appreciable increase in noise temperature; this may be due to lower density of condensed water in the cloud or to smaller thickness along the line of sight. Both of the two exhibited records clearly indicate that the passage of clouds is often associated with an increase in noise brightness temperature of up to 2 °K, and also that the increase and decrease of noise level is directly associated with the intersection of the antenna beam with the edge of the cloud.

b. 3 KMc Observations

The 8 KMc observations described in the previous section were all analyzed by judging the peak-to-peak amplitude of the fluctuation component from the analog records. When an attempt was made to observe the atmospheric fluctuation component at 3 KMc, it was soon found that the atmospheric effect during normal weather conditions was too

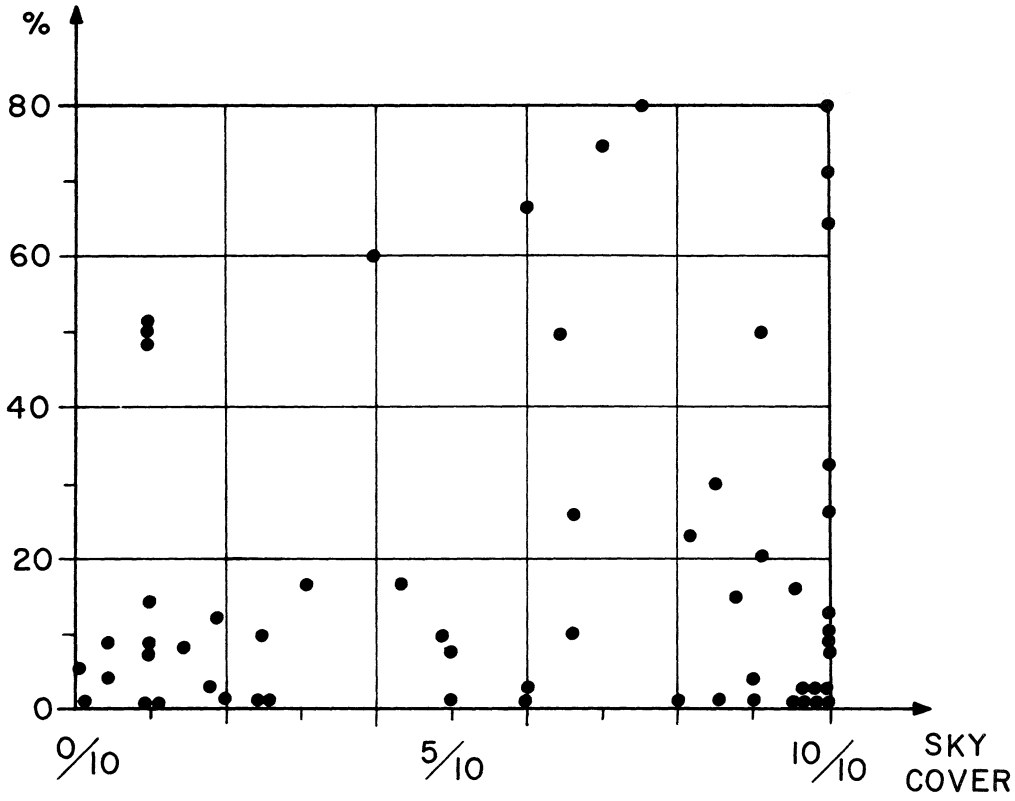

Fig. 24. — The dependence between occurrence of fluctuation and average sky cover.

small to be measured from the analog records. In order to obtain a reliable estimate it was also found necessary to keep a close track on the receiver's performance. This was done by pointing the telescope to ground and observing the output of the receiver for about 20 minutes. Digital output data as well as analog data were simultaneously taken. The atmosphere was then observed by parking the telescope at a fixed zenith angle in the southernly direction and letting the sky drift by. The sky at each zenith angle was observed for approximately 20 minutes. Using a 10-second time constant at the receiver output, the rms-fluctuation can be determined to an accuracy of approximately 5 per cent with the aid of a digital computer. In order to suppress drift and long-term variations, a second-degree least-squares fit was applied to each run. Analysis of the rms-fluctuations of the ground runs (ΔT_G) gave information concerning the receiver stability, and only data which showed negligible or small drift of ΔT_G were treated. A

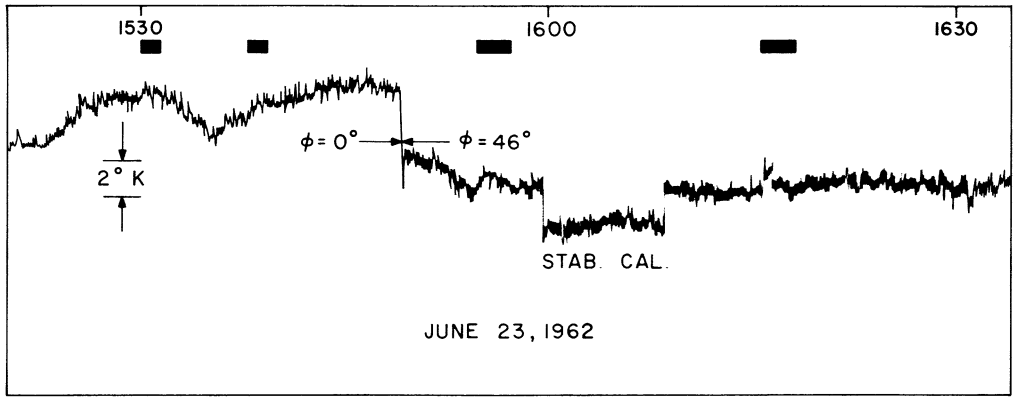

Fig. 25. — Simultaneous observations of sky-noise variations and occurrence of cloud in the direction of the antenna beam, June 23, 1962. Zenith angle ϕ of the antenna is marked on the record.

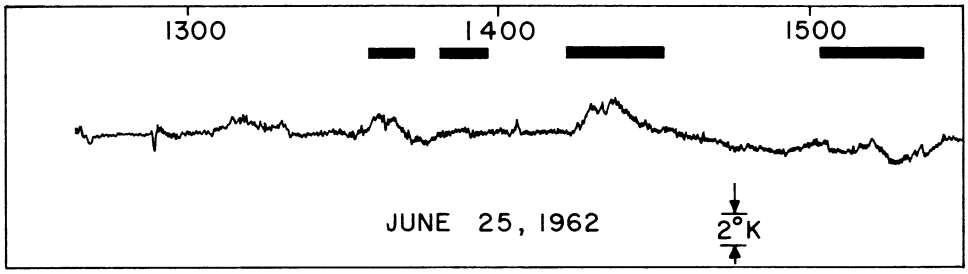

Fig. 26. — Simultaneous observations of sky-noise variations and occurrence of cloud in the direction of the antenna beam, June 25, 1962.

linear approximation was then applied to the variation of ΔT_G, and the quantity

$$\Delta T_A = \left[(\Delta T_G)^2 - (\Delta T_S)^2 \right]^{1/2}$$

was calculated. ΔT_S is the total observed output rms-fluctuations for a sky run and ΔT_A is the rms-value of the fluctuation in antenna temperature, which we assume was due to the atmospheric fluctuation component. The corresponding variation in bright-

ness temperature was then calculated using 60 per cent as the efficiency of the 85-foot telescope at 3 KMc. Figure 27 shows the rms brightness-temperature fluctuation as a function of zenith angle. If we assume that the fluctuations are due to layer-type clouds, for instance, then the fluctuation amplitude would be proportional to sec ϕ. The function $(\Delta T_b)_o$ sec ϕ is also shown on the graph. The zenith fluctuation component $(\Delta T_b)_o$ is assumed to be 0.03 °K. The amount of data is not sufficient to determine whether the zenith angle dependence does, in fact, follow the simple sec ϕ-law. The data indicates however, an increase in ΔT_b for increasing zenith angle. The data represented in Figure 27 were taken in May during the period 0200-0700 when clouds were always present in the direction of the antenna beam.

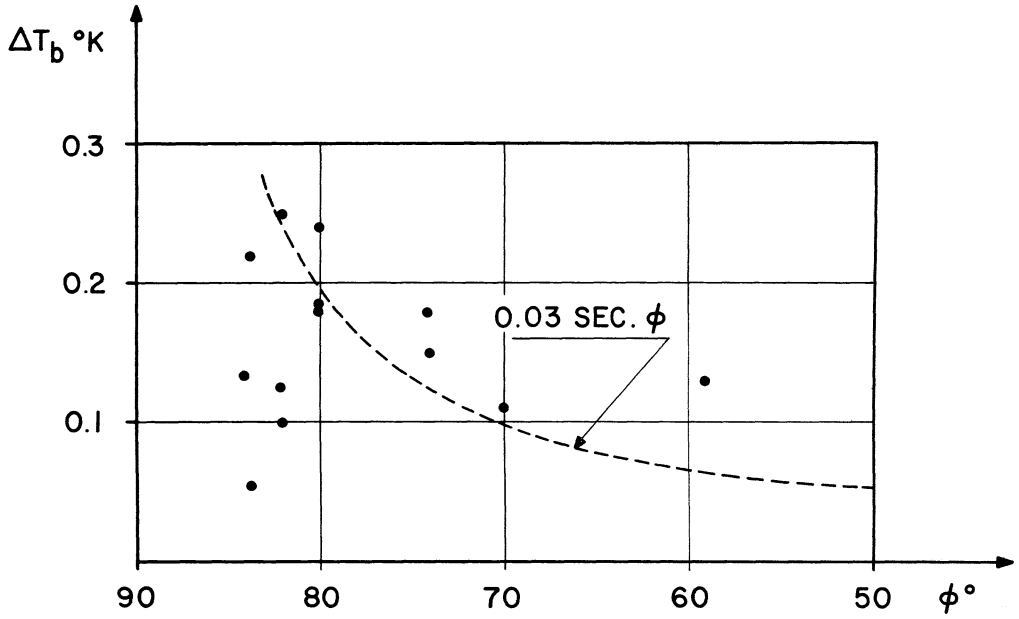

Fig. 27. — Atmospheric fluctuation-noise component at 3 KMc as a function of zenith angle.

A comparison between the 8 KMc and the 3 KMc data cannot be made unless we make an assumption about the ratio of the peak-to-peak and the rms-value for the fluctuation component. Assuming this ratio to be 2, the peak-to-peak values of the 3 KMc fluctuation component at 52° zenith angle is of the order of 0.2 °K. The adoption of a mean value of the 8 KMc component of 1.5 °K (compare Figure 23) gives us a ratio of the 8 KMc

to 3 KMc fluctuation amplitude of 7.5. The wavelength dependence of fluctuations caused by clouds can be shown to approximate closely an inverse square law, giving in our case

$$\frac{(\Delta T_b)_{\lambda = 3.75}}{(\Delta T_b)_{\lambda = 10}} = \left(\frac{10}{3.75}\right)^2 = 7.1 \ .$$

The results of our 8 KMc observations therefore agree very well with the ones to be expected from fluctuations caused by condensed water in clouds.

V. DISCUSSION AND CONCLUDING REMARKS

The results in the preceding section indicated that the brightness temperature of atmospheric radiation has a fluctuation component with a periodicity of the order of minutes. This fluctuation component has been exclusively observed at 8 KMc for 6 1/2 months, while some observations have also been made at 3 KMc. The statistical material of the 8 KMc observations, based on 2000 hours of observations, shows that for the observing parameters used, the fluctuation component exceeded 1 °K brightness temperature on the average of 20 per cent of the total time (Figure 27). The fluctuation component has a positive correlation with average sky cover (Figure 24), although there seems to be a residual fluctuation component when no clouds are present. This point can be seen from the sample records shown (Figure 19). During a day with no visible clouds, the fluctuation of brightness temperature was of the order of 1-2 °K. We can therefore divide the fluctuation component into two parts: one which is caused by clouds drifting through the antenna beam and another which is probably due to variations in the integrated water vapor density in the direction of the antenna beam. A direct correlation with the passage of clouds through the antenna beam is shown in two records (Figures 25 and 26), where noise-temperature variations of up to 2 °K are associated with the cloud passage. These values also agree with the variation in brightness temperature to be expected from average cloud parameters. From the few cases observed, it seems that the periodicity of the noise variation was similar to the one to be expected from clouds of homogeneous medium. This is a point of uncertainty, because if the clouds were of the same angular size as the antenna beam then fine structure details would have been smoothed out. Fine structure is to be expected since refractometer observations within cumulus clouds, for instance, show quite heavy variations in the index of refraction, indicating strong variations in the water vapor density. It should be remembered that the 8 KMc observations were conducted with antennas having beamwidths of the order of 2°. Larger fluctuations are to be expected when antennas having higher resolution are used. The question of the angular size of the atmospheric irregularities producing the fluctuation components is important and experiments should be made in order to determine this parameter.

It was pointed out in Section I that the fluctuation component of the atmospheric noise radiation is of great importance for the sensitivity in radiometric observations. It should, however, be emphasized that only those fluctuations having a periodicity of the same order of magnitude as the output noise fluctuations can seriously affect the sensitivity. Further, the discussion of the effect which the variation in brightness temperature has

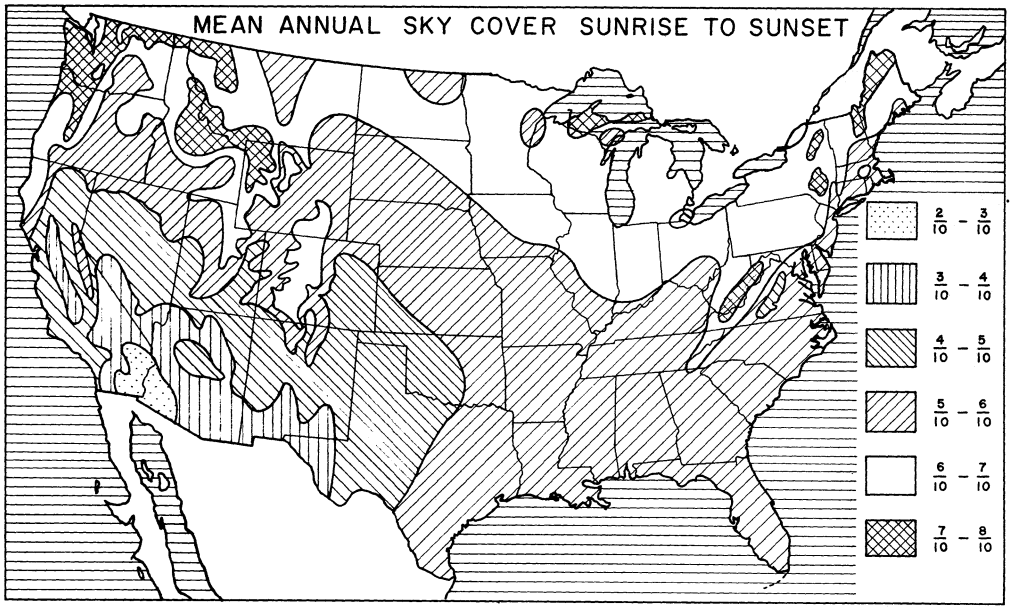

Fig. 28. — Mean annual sky cover for the United States.

upon the system sensitivity has been made by assuming that the antenna system is a single-type telescope. The effect can probably be greatly reduced if a sky-comparison technique is utilized, or if multiple antennas or feeds are used in a correlation receiver of the type introduced by Ryle (1962), where the spatial spectrum of low frequencies are suppressed. The question as to what degree of suppression can be obtained is dependent upon the angular extent of the variable atmospheric component.

The effect of the fluctuation component can also be lowered by proper choice of the observing site. Since the present results have shown a detailed correlation of the fluctuation component with clouds, the average sky cover should be considered.

Figure 28 shows data published by the U. S. Weather Bureau (1961) giving the mean annual sky cover for the U.S.A. The eastern part of the country is dominated by average sky cover of approximately 6/10, but there are also relative small areas close to the east coast having a mean cover as high as 7/10-8/10. Such areas are localized along the Appalachian Mountains in Virginia, West Virginia, New York, Vermont, and Maine. In the western part, on the other hand, the situation is more complex. The area having minimum sky cover (2/10-3/10) is located on the border between southern California and Arizona, but there are also fairly big areas in California, Nevada, Arizona, New Mexico, and Texas having a mean sky cover of 3/10-4/10.

If we assume that the fluctuation component is approximately proportional to the noise level caused by the presence of water vapor, then the variation of the total amount of

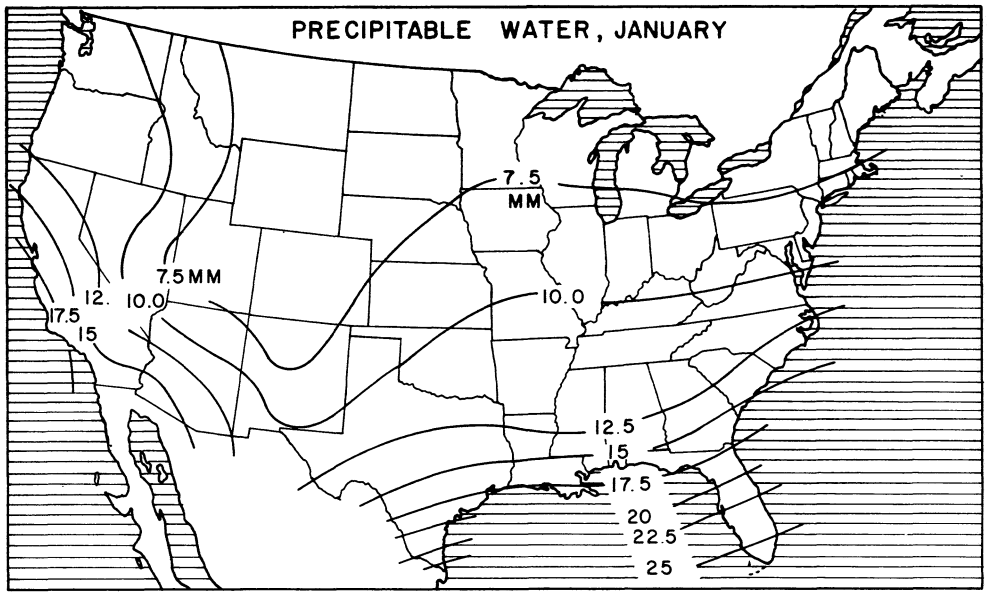

Fig. 29. — Distribution of precipitable water in mm for January. (Calculation made from surface.)

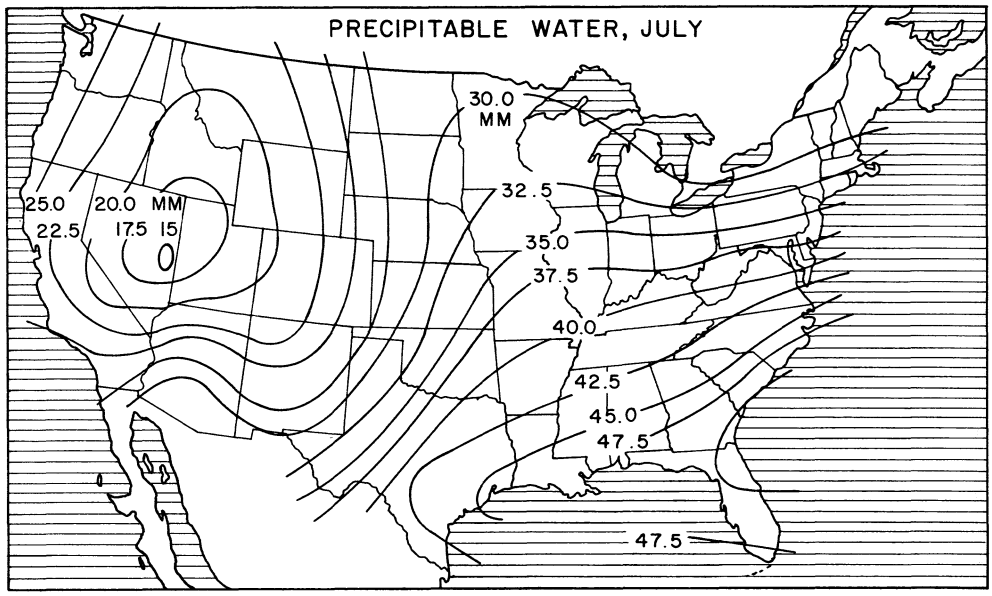

Fig. 30. — Distribution of precipitable water in mm for July. (Calculation made from surface.)

water vapor in a column in the atmosphere is important. Such data have been computed by Shands (1949) and the results for winter and summer are shown in Figures 29 and 30. The two maps show the distribution of the total water vapor content, of the atmosphere, or the precipitable water, expressed in mm. It is obtained by integrating the absolute humidity in an air column from the surface over a cross section of 1 cm^2. There are two components contributing to the value of the precipitable water: one component is dependent upon latitude (compare the situation on the east coast in Figures 29 and 30) and the other component is dependent upon the altitude. (The Rocky Mountain area has the minimum amount of precipitable water.) The former component is directly related to the temperature variation with latitude. The ratio between the maximum and minimum values of the amount of precipitable water is about 3:1 (approximately independent of season) and we should, therefore, expect the fluctuation component due to water vapor to vary approximately in the same way from the worse part to the best part of the country.

The present investigation has shown that the small-scale fluctuation component of atmospheric brightness temperature may be a serious limiting factor at microwave frequencies, and therefore has to be taken into account when high sensitivity is to be achieved in radio astronomy.

The work reported here was initiated by Drs. Findlay and Drake, and their support and encouragement is gratefully acknowledged. The author also acknowledges many helpful discussions with members of the staff. The contribution of Messrs. Kuhlken and Zatta in redesigning and maintaining the radiometer system is gratefully acknowledged.

REFERENCES

Aufm Kampe, H.J., 1950, J. Meteorol., 7, No. 1, 54-57.

Brewer, A.W. and Harrison, A.N. 1944, Meteorol. Res. Conf. Paper, No. 205, Air Ministry, London.

Cole, A.E. 1960, Handbook of Geophysics, Chapter 7, (New York: The Macmillan Co.).

Crawford, A.B., Hogg, D.C., and Hunt, L.E. 1961, Bell System Tech. J., 40, 1095-1116.

Dicke, R.H., Beringer, R., Kyhl, R.L., and Vane, A.B. 1946, Phys. Rev., 70, 340-348.

Drake, F.D. and Ewen, H.I. 1958, Proc. IRE, 46, 53-60.

Gerhardt, J.R. and Crain, C.M. 1955, Proc. Fifth Weather Radar Conf., 43-44.

Gunn, K.L. and East, T.W.R. 1954, Quart. J. Roy. Meteorol. Soc., 80, 522-545.

Hogg, D.C. 1959, J. Appl. Phys., 30, September, 1417-1419.

Hogg, D.C. and Semplak, R.A. 1961, Bell System Tech. J., 40, 1331-1349.

Langille, R.C. 1950, J. Geophys. Research, 55, 51-52.

Ludham, F.H. and Mason, B.J. 1957, Handbuch der Physik, 48, Geophysik II (Berlin, Gottingen, Heidelberg: Springer).

Pawsey, J.L. and Bracewell, R.N. 1955, Radio Astronomy (Oxford: University Press).

Ryle, M. 1952, Proc. Roy. Soc. (London), 211, 351.

Shands, A.L. 1949, Weather Bureau Tech. Paper, No. 10.

U.S. Weather Bureau, 1961, Prepared by Office of Climatology (Washington: U.S. Gov't. Printing Office).

van Vleck, J.H. 1947, Phys. Rev., 71, 425.

Weickmann, H.K. and Aufm Kampe, H.J. 1953, J. Meteorol., 10, No. 3, June, 204-211.
Westerhout, G. 1959, unpublished report.
Zaitsev, V.A. 1950, Glav. Geofiz. Observ., Trudy, 19, 122-132.